ECCD scenarios for different configurations of the W7-X Stellarator

N.B. MARUSHCHENKO, C.D. BEIDLER, V. ERCKMANN, H. MAASSBERG and Yu. TURKIN

Max-Plank-Institut für Plasmaphysik, IPP-EURATOM-Association, 17491 Greifswald, Germany

October 15, 2007

In order to avoid significant change of the edge value of the rotational transform in the W7-X stellarator, electron cyclotron current drive (ECCD) will be used for compensating the bootstrap current (an ohmic transformer is absent). Since ECCD efficiency is quite sensitive not only to the plasma parameters, but also to the magnetic configuration, it is an important task to estimate properly the range of ECCD values taking into account all features of the magnetic configuration, and to assess its ability to counteract the residual bootstrap current. In this work we analyze the requisite ECCD for scenarios with the different magnetic configurations with help of the ray-tracing code TRAVIS, coupled self-consistently with the 1D transport code. The neoclassical transport modeling is based on the DKES database of mono-energetic transport coefficients.

Keywords: stellarator, bootstrap current, electron cyclotron heating, current drive

1. Introduction

The W7-X stellarator (under construction in Greifswald, Germany) is a large-scale device with average major radius $R_0 \simeq 5.5$ m and plasma radius $a \simeq 0.53$ m, equipped with superconducting coils, with a low-shear configuration of the Helias (Helical Advanced Stellarator) type [1] with five field periods. The toroidal mirror ratio $B_{\max}/B_{\min}$ on axis can be varied significantly, from 1.004 to 1.22 for the "low-mirror" and the "high-mirror" configurations, respectively (for the "standard" configuration $B_{\max}/B_{\min} = 1.09$). The corresponding trapped-particle fractions on axis are varied due to ripples from $f_{\rm tr} \simeq 0.02$ for "low-mirror" up to $f_{\rm tr} \simeq 0.45$ for 'high-mirror", while $f_{\rm tr} \simeq 0.3$ for the "standard" configuration. Through its dependence on the toroidal mirror ratio value, mono-energetic bootstrap current coefficients are largest for the "low-mirror" configuration. In particular, the bootstrap current is minimized for the "high-mirror" configuration, whereas the neoclassical confinement is optimum in the "standard" configuration. The total plasma current affects the edge value of the rotational transform, which may fall outside the required range for proper island divertor operation without external field compensation. Due to the absence of an ohmic transformer, electron cyclotron current drive (ECCD) will be used for compensating the bootstrap current. Since the ECCD efficiency is quite sensitive not only to the plasma parameters, but also to the magnetic configuration, it is an important task to estimate properly the range of ECCD values taking into account all features of the magnetic configuration, and to check its ability to counteract the residual bootstrap current. It is necessary to take special care for high densities where the ECCD efficiency is reduced. Additionally, the effects of finite plasma pressure ($\beta > 0$) may play a significant role, especially in the high-density scenarios, changing the deposition and current drive profiles. Since the task of self-consistent simulation of this case is still too complex, the effects of finite β will be only briefly discussed (when it is possible), just to indicate the tendency.

author's e-mail: nikolai.marushchenko@ipp.mpg.de

2. W7-X ECRH system and ECCD scenarios

The ECRH system in W7-X is designed for continuous operation with a total injected power up to 10 MW at 140 GHz [2] (the resonance magnetic field is $B_0 = 2.5$ T). The ports for launching the RF power are situated symmetrically around two "bean-shaped" planes, i.e. near the maximums of B (the ports E10 and A51 near the cross-sections $\phi = 0$ and $\phi = 72°$, respectively). In order to prevent an overheating of the chamber by the shine-through power and to control its reflection, mirrors are installed at the inner wall and all beams planned for O2 operation must be directed to these mirrors. Because of symmetrical location of the mirrors about the launch ports, only five beams out of ten can be launched in the same direction, and operation with maximal counter-ECCD is possible with a total power up to only 5 MW. While the X2 (extra-ordinary mode at the 2nd harmonic) scenario is applicable in the density range $n_e < 1.2 \times 10^{20}$ m^{-3}, for higher densities, up to 2.2×10^{20} m^{-3}, the O2 (ordinary mode at the 2nd harmonic) scenario will be applied. Note, that for densities near the O2 cut-off, $n_e \simeq 2.4 \times 10^{20}$ m^{-3}, single-pass absorption of the O2-mode is strongly reduced together with increasing refraction effects, the upper density limit for operation is about $n_e \simeq 2.2 \times 10^{20}$ m^{-3} (or even less, depending on the specific case). Due to the high optical thickness of the plasma for the X2-mode, there are no strict launch conditions for this scenario, and this freedom can be used for tailoring a desired deposition and current drive profile

[3]. For the O2-mode, the plasma is optically "gray", and this scenario is more limited for the expected range of parameters. Since the optical depth for the O2-mode scales as $\tau_{O2} \propto T_e^2$, the most attractive path to the O2 scenario is to preheat the plasma by the X2-mode, then change the polarization from X- to O-mode by means of rotation of the corrugated mirrors, and finally to increase the density to the requested value [4, 5].

Below we consider in detail both ECCD scenarios, with the X2-mode for the moderate density range, $n_e < 10^{20}$ m^{-3}, and with the O2-mode for the higher densities. To simplify comparison of the X2 and O2 scenarios, the launch conditions for the X2-mode are taken identical to those required for the O2-mode.

3. Numerical tools

The numerical models for calculating the ECCD efficiency developed to date (both the Fokker-Planck [6] calculations and the adjoint approach [7] in ray-tracing calculations) do not cover completely the range of collisional regimes for the electrons involved in the current drive, especially in stellarators. Only two opposite limits are in use, with and without taking into account the trapped particles. The first one, called the collisional limit, is formulated under the condition $\nu_e \gg \tau_b^{-1}$, where ν_e and τ_b are the electron collision frequency and the bounce-time, respectively. This limit, being, in fact, the straight magnetic field line approach, overestimates the ECCD efficiency. The second limit, called the collisionless one, is based on the opposite assumption, $\nu_e \ll \tau_b^{-1}$, i.e. takes into account the trapped particles. This limit may lead to underestimating of the ECCD efficiency. Nevertheless, the collisionless limit is more reasonable for the W7-X conditions, especially for the regimes with moderate densities and high temperatures. In this work we analyze the requisite ECCD scenarios for operating with the different magnetic configurations with help of the ray-tracing code TRAVIS [8, 9]. The (adjoint) Green's function applied for the ECCD calculations is formulated with momentum conservation taken into account [4]; this is especially important and even critical for those scenarios, where the number of trapped particles is quite small, $f_{\rm tr} \ll 1$, and/or mainly bulk electrons are responsible for absorption of the RF power (e.g. when the obliqueness of launch is not high and $N_\parallel \ll 1$).

The plasma profiles and bootstrap current were calculated by the 1D transport code [5] (for details, see also [10]) coupled self-consistently with the ray-tracing code TRAVIS [8, 9]. The transport modeling is based on the DKES database of mono-energetic transport coefficients, and thermal transport coefficients are obtained by energy convolution with a local Maxwellian. The DKES code [11] uses as collision operator the Lorentz pitch-angle scattering term without momentum conservation, leading to an overestimate of the bootstrap current depending on $Z_{\rm eff}$ (in present the calculations, $Z_{\rm eff} = 1.5$ is assumed).

4. Simulation results

The calculations were done for five different beams launched from the ports E10 and A51 with 1 MW power for each beam. Both X2 and O2 scenarios are modeled for the same fixed launch conditions for three different magnetic configurations. While the RF-beams in O2 scenarios must be directed onto the corresponding mirrors at the inner wall, the chosen direction is not optimal for ECCD efficiency in X2-mode. Since the single-pass absorption of the O2-mode is less than 100%, four passes are taken into account in the calculations. If after two passes through the plasma less than 90% of the power was absorbed, this scenario was excluded from consideration.

Keeping in mind the general scenario which requires switching from the X2 to the O2 scenario, let us consider first the moderate density range, $n_e \lesssim 10^{20}$ m^{-3}, where both scenarios can work. For the present conditions, the choice $B = 2.562$ T seems as optimum for both X2 and O2 scenarios. For the X2 scenario, an off-axis absorption does not lead to the "electron-root" feature and collisional decoupling of electrons and ions. For the O2 scenario, due to the shift of the resonance in the low-field-side direction, absorption appears in the region of increasing (along the ray) T_e, prolonging the area of effective cyclotron interaction and, consequently, increasing the single-pass absorption.

In Fig.1 (top), the X2 ECCD profiles, $j_{cd}(\rho)$, which summarize the contributions from all beams, are shown (the corresponding deposition profiles have a very similar shape). Negative ECCD is chosen since the bootstrap current is positive for these simulations. Due to very high optical thickness, the location of the deposition profile (ECCD as well) for the X2-mode is almost completely defined by the resonance location, and the Doppler broadening is mainly responsible for the width of $j_{cd}(\rho)$ profile. For each configuration, the temperature dependence during the density scan is not strongly pronounced due to an absence of its strong variation: for the "standard" configuration with n_e increased from $0.4{\times}10^{20}$ m^{-3} to $1.1{\times}10^{20}$ m^{-3}, T_e is varied from 5.7 keV to 4.4 keV, respectively. Since the "standard" configuration is optimized for neoclassical confinement, the steady-state temperature obtained by transport simulation is highest in comparison with the "low-" and "high-mirror" configurations. On the other hand, due to the reduced trapped particle fraction, the longitudinal conductivity is higher in the "low-mirror" configuration, which leads to an increase of ECCD. Nevertheless, due to the reduced confinement the temperature in the "low-mirror" configuration is for the same heating conditions also lower, and the decrease of $f_{\rm tr}$ is masked by a decrease of T_e. In the case of the "high-mirror" configuration, an increase of $f_{\rm tr}$ and a decrease of T_e have the same effect, and the ECCD efficiency is significantly reduced. For comparison, the case of the "standard" configuration with $\langle\beta\rangle = 0.02$ is shown (see Fig.1, dashed red). One can see, that the finite pressure effects may lead to a very strong effect. Due to the

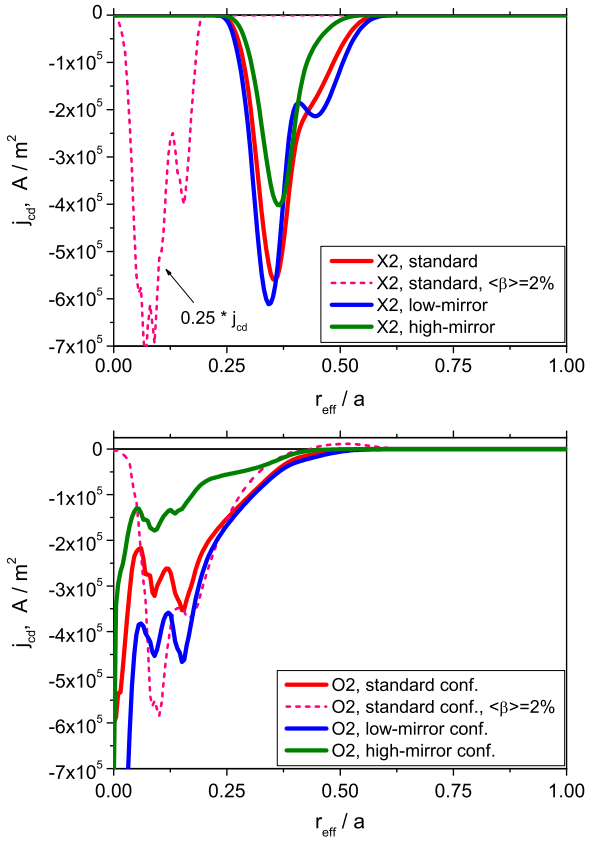

Fig. 1 Summarized ECCD profiles (5 beams 1 MW each) for the different configurations: "standard" (red), "low-mirrors" (blue), and "high-mirrors" (green). Additionally, the case of $\langle\beta\rangle = 0.02$ for the "standard" configuration is shown (pink dashed). Top - X2 scenario, bottom - O2 scenario. For all cases, the density is the same, $n_e = 0.8\times10^{20}$ m^{-3}.

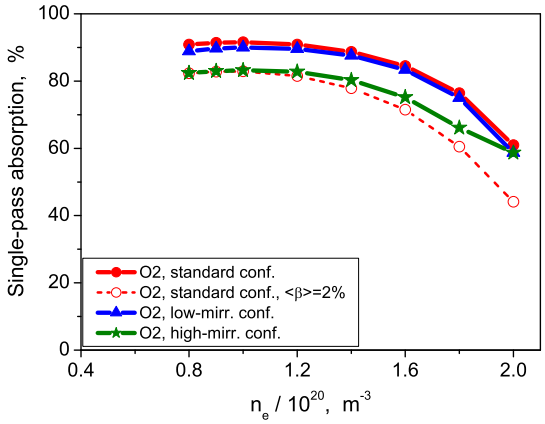

Fig. 2 Single-pass absorption of the O2-mode summarized for all beams: the same as in Fig.1.

Shafranov shift combined with the diamagnetic effect, the deposition profile (ECCD as well) moves into the axial region, making an appearance of the "electron-root" almost unavoidable.

The O2 scenario is more sophisticated. First of all, the plasma is optically "gray" and a significant part (up to 20% or even more) of the power is absorbed during the second pass (third and fourth passes are of minor importance). Direct consequence of it is involving in cyclotron interaction the electrons with $k_\parallel v_\parallel < 0$ ("anomalous" Doppler effect), which create the current contribution of opposite sign, reducing $j_{cd}(\rho)$ in this point [7]. Interesting, that for the "standard" configuration with $\langle\beta\rangle = 0.02$ this effect is most pronounced, and even negative values of $j_{cd}(\rho)$ appear (see Fig.1, bottom, red dashed). Important to mention also, that despite of launching the RF beams near the maximum of B ("bean-shaped" plane) the trapped particles are quite well involved in the cyclotron interaction, absorbing up to 10% of the power and significantly reducing the ECCD. The absorption of the O2-mode, being proportional to T_e^2, is very sensitive to the shape of T_e profile (n_e profile is almost flat in the present simulations). On the other hand, the T_e profile is defined mainly by the deposition profile. Due to this feedback, the resulting deposition profiles (as well as ECCD) for the scenarios with the resonance shifted to the low-field-side are rather independent of density, and its shape is quite similar to those shown in Fig.1 (bottom) for quite broad range of densities (with only change of $j_{cd}(\rho)$ magnitude, which scales roughly as $1/n_e$).

In the Fig.2, the single-pass absorption for the O2 scenario as a function of density is shown. The values obtained (summation over five beams) are quite high for all tested magnetic configurations, i.e. are about 80 - 90% for $n_e < 1.8\times10^{20}$ m^{-3}. Important to mention here, that the single-pass absorption in the "standard" magnetic configuration with $\langle\beta\rangle = 0.02$ is significantly reduced in comparison with the vacuum configuration (compare the red solid and pink dashed lines). As was mentioned above, this effect is due to a combination of the Shafranov shift and of the diamagnetic effect, which leads, in fact, to shifting of the deposition profile into the high-field-side direction, reducing the optical depth.

In Fig.3, the results of the density scan for the three magnetic configurations are shown. Following the standard theoretical predictions, the current drive for both X2- and O2-mode scales roughly as $1/n_e$. As expected, the current driven by X2-mode is larger than that of the O2-mode for all tested configurations. There are three main factors which lead to this jump of ECCD efficiency (from red circles to red triangles). First, the single-pass absorption of the O2-mode is less than 90%, and the rest of the power is absorbed in the plasma periphery, where the temperature is low. Second, since the deposition profile is quite broad, both the "anomalous" Doppler effect and the participation of the trapped particles in the cyclotron interaction reduce the ECCD efficiency.

The bootstrap current can be compensated by X2-ECCD for the "high-mirror" and "low-mirror" configurations (in the last case, the uncompensated residual current appears acceptable). For the "standard" configuration (apart from the lower densities), this compensation can be

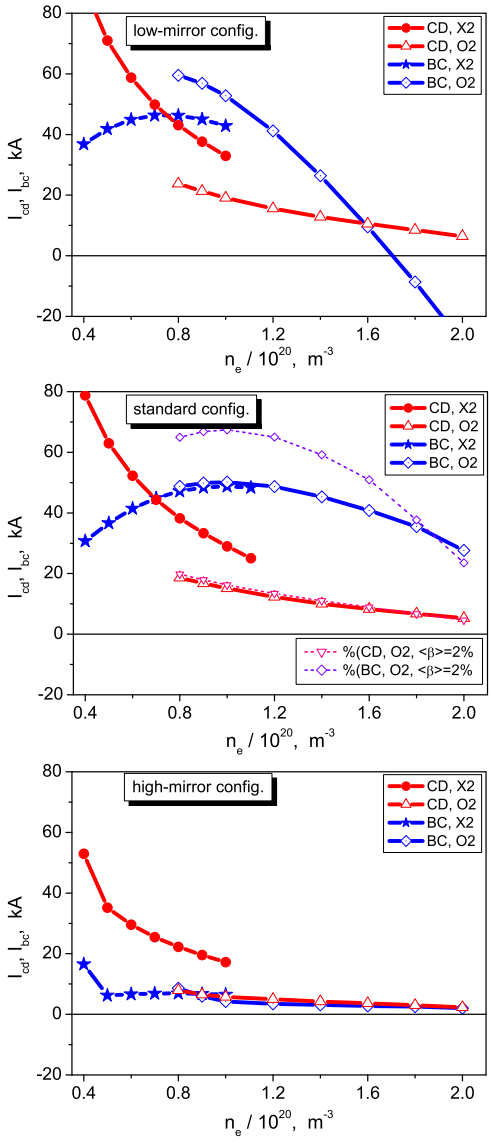

Fig. 3 Density scan for different magnetic configurations. Both I_{cd} (red color, circles for X2 and triangles for O2 scenarios) and I_{bc} (blue color, stars for X2 and rectangles for O2 scenarios, respectively) are shown.

done by further optimization of the launch conditions (in the present study, all beams are directed onto the mirrors, although this is not necessary). Full current control at high density (in operation with O2-mode) is only obtained for the "high-mirror" configuration. Note, that for the "standard" configuration with $\langle\beta\rangle = 0.02$, the bootstrap current is significantly increased, while the ECCD is almost unchanged. This problem requires additional study.

5. Discussion

In the present paper, the results of numerical simulations of different ECCD scenarios for W7-X are presented, the X2 scenario, which is applicable for the low and moderate density range, $n_e < 1.2 \times 10^{20}$ m^{-3}, and the O2 scenario for higher densities up to $n_e < 2.2 \times 10^{20}$ m^{-3}. Three different magnetic configurations have been tested, with the trapped particle fraction varied from 1.004 to 1.22. The aim of this study was to estimate the ability of the ECRH system of W7-X for compensating the residual bootstrap current and to control the edge value of the rotational transform.

In high-density operation at low ECRH power, the bootstrap current might exceed the maximum ECCD both for the X2- and the O2-scenarios. Only the "high-mirror" configuration was shown to have rather small bootstrap currents thus confirming the corresponding W7-X optimization criterion. For the "standard" configuration with improved neoclassical confinement, however, ECCD control of the bootstrap current is only possible in X2-mode at lower density. With full current control by ECCD, only a few skin-times (i.e. less than 10 sec) are necessary to obtain stationary conditions for optimum divertor operation.

High density scenarios are also important for the W7-X island divertor operation since fairly high separatrix densities (about 0.4×10^{20} m^{-3}) are required. Consequently, the O2-scenarios are expected to be very important for longer discharges. For these conditions, however, only the "high mirror" configuration allows for bootstrap current control by ECCD. In particular for the "standard" configuration, another discharge scenario must be chosen to obtain stationary conditions. Here, the edge value of the rotational transform in the vacuum configuration must be reduced by the amount which is generated by the bootstrap current in the final steady state. The discharge is operated at low density and rather low heating power with strong co-ECCD (in X2-mode) up to roughly stationary plasma current, i.e. the desired island divertor configuration is reached. In this scenario, however, the evolution of the plasma current scales on the L/R-time (i.e. several 10 sec). Then, the density as well as the heating power can be ramped up and the co-ECCD is reduced with the increasing bootstrap current, i.e. the total current is controlled. The internal current densities and the ι-profile become stationary again on the skin time. Such a discharge scenario, however, is much more complex compared to the case of full ECCD control of the bootstrap current.

[1] J. Nührenberg and R. Zille, Phys. Letters **114A** (1986) 129
[2] V. Erckmann *et al.*, Fusion Sci. and Technol. **52** (2007)
[3] H. Maassberg *et al.*, Plasma Phys. Control. Fusion **47** (2005) 1137
[4] M. Romé *et al.*, Plasma Phys. Control. Fusion **40** (1998) 511
[5] Yu. Turkin *et al.*, Fusion Sci. and Technol. **50** (2007) 387
[6] C.F.F. Karney, Comp. Phys. Reports **4** (1986) 183
[7] M. Taguchi, Plasma Phys. Control. Fusion **31** (1989) 241
[8] N.B. Marushchenko *et al*, 2006 Proc. of 14th Joint Workshop Electron Cyclotron Emission and Electron Cyclotron Heating, Santorini, Greece, May 9-12, 2006, http://www.hellasfusion.gr/ec14/papers/26.pdf
[9] N.B. Marushchenko *et al* 2006 Proc. of 16th Toki Conference, Toki, Japan, December 5-8, 2006, http://itc.nifs.ac.jp/index.html
[10] Yu. Turkin *et al.*, this conference, P2-064
[11] W.I. van Rij and S.P. Hirshman, Phys. Fluids B1 (1989) 563